MODELING CARBON PRODUCTION AND DENSITIES IN THE MARTIAN ATMOSPHERE UNDER MAVEN DEEP DIP 2 CONDITIONS. D. Y. Lo[1], R. J. Lillis[2], R. V. Yelle[3] and the MAVEN team, [1]Lunar and Planetary Laboratory, University of Arizona. Tucson, AZ USA, [2]Space Sciences Laboratory, University of California. Berkeley, CA USA, [3]Lunar and Planetary Laboratory, University of Arizona. Tucson, AZ USA.

Introduction: Ancient Mars is believed to have had a thicker atmosphere of >200 mbar of CO_2 in order to have supported extensive surface standing water [1–5]. Exactly how the CO_2 was removed from the atmosphere over the last 3.6 Gyr to the present ~6 mbar remains a mystery. With carbonate sequestration at the surface accounting for only a maximum of ~12 mbar [6], escape into space seems to be the dominant loss pathway. Loss of CO_2 into space involves first photochemical conversion of CO_2 into atomic C and O, which are then separately lost through photochemical, pickup or sputtering processes. Observations of present H and O loss rates at a ratio of ~2:1 by the Mars Atmosphere Volatile EvolutioN (MAVEN) spacecraft hint at the dominant role of H_2O [7], deepening the mystery of how substantial C can escape without a corresponding 2x escape of O.

The first step to understanding C loss rates over the history of Mars is to understand the various controls behind C densities and production today. Several important developments have occurred since the last models studying C densities in the Martian atmosphere. CO_2^+ dissociative recombination (DR) as a production channel for atomic C, first proposed by [8] and explored in detail by [9] based on rate measurements by [10], has been shown to be negligible with further measurements by [11]. On the other hand, rates of the previously theoretical $CO_2 + h\nu \rightarrow C + O_2$ have now been experimentally measured by [12]. Finally, the MAVEN mission [13] has now returned comprehensive maps of neutral, ion and electron densities of the Martian upper atmosphere, providing us with an empirical foundation that is of better quality and has better coverage than the limited Viking lander atmospheric profiles for modeling photochemistry in the Martian atmosphere.

Model Description: We use a global-averaged 1-D neutral-ion model to investigate the photochemistry spanning altitudes 0–240 km in the Martian atmosphere. The model tracks the densities of 34 neutral species and 34 ionic species as they undergo photochemical reactions (247 neutral, 583 ion, 20 electron impact and 53 photodissociation reactions) and diffusion (both eddy and molecular). Boundary conditions are set for each species. The model is then run forward with timesteps of various sizes to ensure that species with various photochemical lifetimes have sufficiently converged. Of particular note, the model makes use of high-resolution (10^{-14} m) CO photolysis cross-sections from Heays to accurately characterize the pre-dissociating states.

Model Inputs: We draw the majority of the model inputs from observations conducted by various instruments on the MAVEN spacecraft during the Deep Dip 2 campaign (18–22 April 2015, L_s = 328°), during which the spacecraft periapse altitude was lowered to 130 km, allowing in situ sampling from the exosphere downward to near the homopause. Deep Dip 2 sampled near the subsolar region (local time ~12 hours, solar zenith angle ~9°), close to the equator and at all longitudes.

Solar fluxes and electron energy distributions used in the model represent an average of observations by the MAVEN Extreme UltraViolet Monitor (EUVM) [14] and Solar Wind Electron Analyzer (SWEA) [15] respectively. The neutral temperature profile is derived from observations by the Neutral Gas and Ion Mass Spectrometer (NGIMS) [16], while the electron temperatures are based on observations by the Langmuir Probe and Waves (LPW) instrument [17]. Averaged density profiles for CO_2, N_2 and Ar from NGIMS are used. He densities are from an extrapolation of [18]. H_2O abundance in the Martian atmosphere is highly seasonal, increasing by 2 orders of magnitudes during the dustier period around perihelion. To account for this seasonal effect, we constructed average "wet" and "dry" profiles from the Mars Climate Database [19–21]. All other species are allowed to equilibrate through photochemistry and diffusion. All neutral species, except H and O, have boundary conditions of zero surface and escape fluxes. H and O have zero surface fluxes, with Jeans and 10^7 cm^{-2} s^{-1} escape fluxes respectively. Boundary conditions for ions are set to be at chemical equilibrium at the surface with zero escape.

Results: In the Martian atmosphere, C is known to be produced from CO_2 and CO. We use our photochemical model to determine the equilibrium C density in the MAVEN Deep Dip 2 atmosphere, and the contribution of each production channel at different altitudes.

1. CO_2 photodissociation and HCO^+ dissociative recombination are significant C production channels (Figure 1). Our model found that the recently discovered CO_2 photodissociation is among the most significant production channels for C, comparable to the previously known top channel of CO photodissociation. We also found a previously unreported third significant production pathway, with HCO^+ DR being the final step:

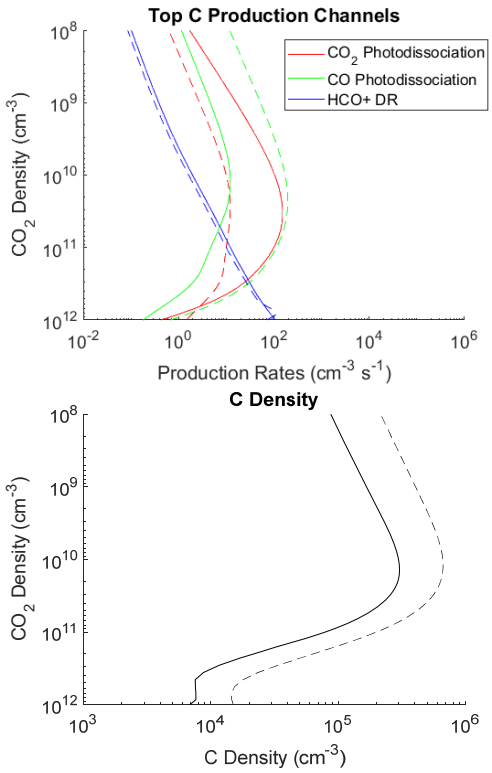

Figure 1: (above) top C production channels, (below) equilibrium C densities with equilibrated CO (solid) and 10x equilibrated CO (dashed) densities.

$$CO_2 \rightarrow CO_2^+ + e \quad (1)$$
$$CO_2^+ + H \rightarrow HCO^+ + O \quad (2)$$
$$HCO^+ + e \rightarrow C + OH \quad (3)$$
$$CO_2 + H \rightarrow C + OH + O$$

Thus, HCO^+ DR, similar to CO_2 photodissociation, provides a pathway for converting CO to C. However, HCO^+ DR contributes only to the thermal C population, producing C atoms with maximum velocity of 2 km/s, less than the escape velocity of 5 km/s.

2. C density increases with CO density. Mars photochemical models currently have problems reproducing observed CO abundances, with model densities typically being lower by ~8x [22]. Our model has a similar limitation. In order to overcome this limitation and study how CO densities control C densities, we investigated a scenario where we fix CO densities to a more realistic (and convenient) 10x higher. Doing so gives ~2x higher C densities (Figure 1), driven by a large increase in CO photodissociation balanced by smaller decreases in CO_2 photodissociation and HCO^+ DR rates.

3. H_2O abundance does not significantly change C densities. Surprisingly, an increase in H_2O abundance did not significantly suppress CO densities through a strengthening of HO_x chemistry. As a result, production of C from CO_2 and CO photodissociation remains similar. While higher H densities under "wet" conditions increase HCO^+ DR rates, loss of C from recombination with O_2 is also faster with the higher O_2 densities associated with "wet" conditions, resulting in similar C densities overall (Figure 2).

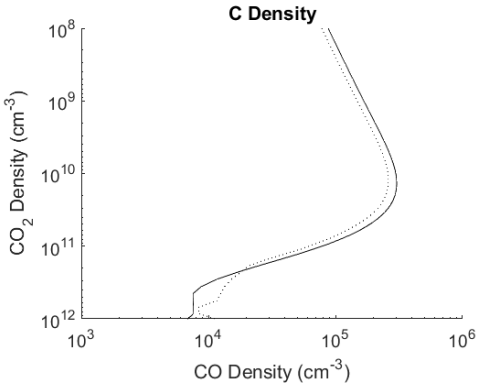

Figure 2: equilibrium C densities for "wet" (dotted) and "dry" (solid) H_2O profiles.

References: [1] Wordsworth R. et al. (2013) *Icarus, 222*, 1–19. [2] Forget F. et al. (2013) *Icarus, 222*, 81–99. [3] Mischna M. A. et al. (2013) *JGR, 118*, 560–576. [4] Richardson M. I. and Mischna M. A. (2005) *JGR, 110*, 1–21. [5] Wordsworth R. D. et al. (2017) *GRL*. [6] Edwards C. S. and Ehlmann B. L. (2015) *Geology*. [7] Jakosky B. M. et al. (2017) *submitted to JGR*. [8] McElroy M. B. and Donahue T. M. (1971) *JGR, 76*(28), 6674–6690. [9] Fox J. L. (2004) *JGR, 109*, A08306. [10] Seirsen K. et al. (2003) *Physical Rev. A, 68*(2), 022708. [11] Viggiano A. A. et al. (2005) *J. Chem. Phys, 122*(22), 10–13. [12] Lu Z. et al. (2014) *Science*, *346*, 6205, 61–64. [13] Jakosky B. M. et al. (2015) *Space Sci. Rev, 195*, 3–48. [14] Eparvier F. G. et al. (2015) *Space Sci. Rev, 195*, 293–301. [15] Mitchell D. L. et al. (2016) *Space Sci. Rev, 200*, 495–528. [16] Mahaffy P. et al. (2015) *Space Sci. Rev, 195*, 49–73. [17] Andersson, L. et al. (2015) *Space Sci. Rev, 195*, 173–198. [18] Krasnopolsky V. A. and Gladstone G. R. (2005) *Icarus, 176*(2), 395–407. [19] Forget, F. et al. (1999) *JGR, 104*(E10), 24155–24176. [20] Millour, E. et al. (2015) *EPSC, 10*, 438. [21] Navarro T. et al. (2005) *JGR, 119*(7), 1479–1495. [22] Lefevre F. and Krasnopolsky V. (2017) in *The Atmosphere and Climate of Mars*, Haberle R. M. et al. (ed.).